

Site-Specific In Vivo Bioorthogonal Ligation via Chemical Modulation

Heebeom Koo, Jeong Heon Lee, Kai Bao, Yunshan Wu, Georges El Fakhri, Maged Henary,* Seok Hyun Yun,* and Hak Soo Choi*

A critical limitation of bioorthogonal click chemistry for in vivo applications has been its low reaction efficiency due to the pharmacokinetic barriers, such as blood distribution, circulation, and elimination in living organisms. To identify key factors that dominate the efficiency of click chemistry, here a rational design of near-infrared fluorophores containing tetrazine as a click moiety is proposed. Using *trans*-cyclooctene-modified cells in live mice, it is found that the in vivo click chemistry can be improved by subtle changes in lipophilicity and surface charges of intravenously administered moieties. By controlling pharmacokinetics, biodistribution, and clearance of click moieties, it is proved that the chemical structure dominates the fate of in vivo click ligation.

1. Introduction

Copper-free click chemistry is ideal for in vivo bioorthogonal reactions due to its fast and facile chemical process with little cellular toxicity.^[1] Despite its potential in bioimaging and nanomedicine including optical imaging,^[2] positron emission tomography (PET),^[3] single-photon emission computed tomography (SPECT),^[4] ultrasound imaging,^[5] and drug delivery,^[6] in vivo click chemistry in the past decade has suffered from relatively low reaction efficiency. This problem has

been attributed in part to the binding of serum proteins to click components. In addition, the pharmacokinetic barriers, such as blood distribution, circulation, and elimination as well as biodistribution and clearance, make it difficult for the click moieties to reach a target.^[7] To improve the click efficiency in vivo, the Weissleder et al. introduced large molecular weight polymers, which increased the circulation time of click moieties in the blood vessels and eventually improved click reaction efficiency.^[7] Although polymer-modified tetrazine (Tz) components facilitated the cycloaddition reaction with the counterpart *trans*-cyclooctene (TCO) by giving enough

reaction time at high concentration, this approach could result in high background retention and limited transportation through the physiological barriers (e.g., blood-brain/nerve barriers and endothelial/intestinal walls).^[8] Thus, small molecules are still attractive for in vivo reactions due to their rapid secretion rates and low potential side effects.^[9] However, the key factors regulating in vivo click chemistry of small molecules have not been fully understood.

Previously, we have studied the pharmacokinetics of nanoparticles and small molecules in various animal models, and defined the physicochemical properties such as size, surface charge, and lipophilicity that play a key role in targeting and imaging.^[10] Very recently, we have developed a novel concept of targeted contrast agents (i.e., structure-inherent targeting), where the inherent chemical structure governs the fate of an injected molecule and the ultimate targeting to specific organs such as thyroid/parathyroid glands,^[10] bone,^[11] and cartilage.^[12] Using this concept, we could achieve significantly reduced background tissue retention and nonspecific uptake in the reticuloendothelial system, and thus improve the signal-to-background ratio (SBR) of the target.^[10,13] Armed with this strategy, we hypothesized that the efficacy of bioorthogonal chemistry in vivo would be largely dependent on the inherent chemical structure of systemically administered molecules, where biodistribution and pharmacokinetics need to be controlled.

Herein, we describe a series of novel pentamethine near-infrared (NIR) fluorophores composed of three main domains: (1) Tz for click chemistry, (2) pentamethine core for NIR fluorescence imaging, and (3) variable charges for pharmacokinetic modulation (Figure 1). The Tz-containing NIR fluorophores were rationally designed to have assorted side groups (R¹ and R²) with varying charges by two, resulting in diverse lipophilicity (Figures S1–S3, Supporting Information). We selected

Prof. H. Koo, Prof. S. H. Yun
Wellman Center for Photomedicine
Massachusetts General Hospital
and Harvard Medical School
65 Landsdowne St., UP-5, Cambridge, MA 02139, USA
E-mail: syun@hms.harvard.edu

Prof. H. Koo
Department of Medical Lifescience
College of Medicine
The Catholic University of Korea
Seoul 06591, South Korea

J. H. Lee, Prof. K. Bao, Prof. G. El Fakhri, Prof. H. S. Choi
Gordon Center for Medical Imaging
Division of Nuclear Medicine and Molecular Imaging
Department of Radiology
Massachusetts General Hospital and Harvard Medical School
Boston, MA 02114, USA
E-mail: hchoi12@mgh.harvard.edu

Dr. Y. Wu, Prof. M. Henary
Department of Chemistry
Center for Diagnostics and Therapeutics
Georgia State University
Atlanta, GA 30303, USA
E-mail: mhenary1@gsu.edu

DOI: 10.1002/adhm.201600574



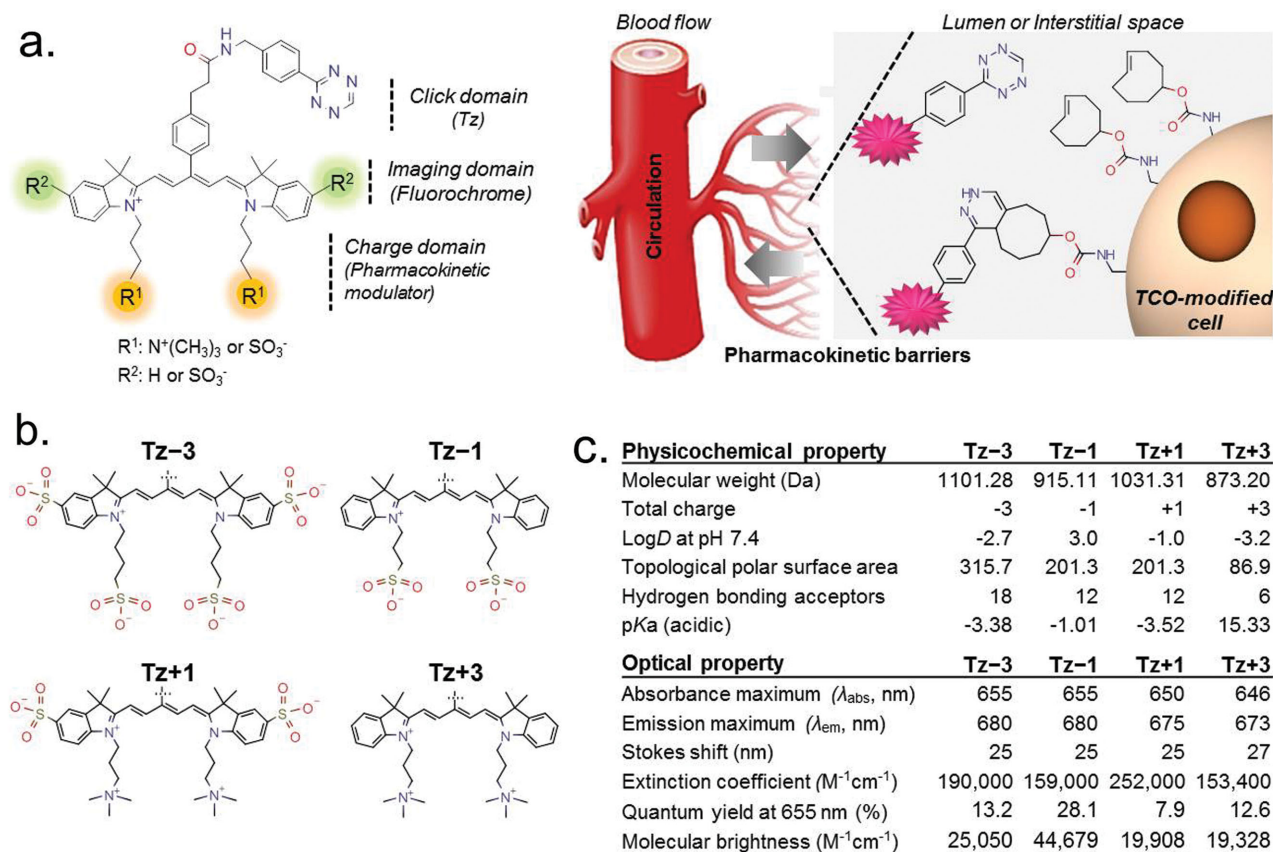


Figure 1. Synthesis of Tz-containing NIR fluorophores to analyze the reaction efficiency of in vivo click chemistry on the TCO-modified cell surface. a) Composition of Tz-containing pentamethine fluorophores and their subsequent click reactions in vivo. b,c) Chemical structures (b) and physicochemical properties (c) of Tz-fluorophores.

these structurally diverse Tz moieties to investigate the reaction efficiency of in vivo click chemistry with TCO presenting on the cell surface.

2. Results and Discussion

We modified surface charges of the pentamethine core to obtain the final Tz-fluorophores with distinctive physicochemical properties such as logD at pH 7.4 (distribution coefficient), TPSA (topological polar surface area), HBA (hydrogen bond acceptor), and pKa (acid dissociation constant). Compounds 4 with assorted charges were conjugated to amine-functionalized Tz through the conventional *N*-hydroxysuccinimide (NHS) chemistry, and the final products were characterized by liquid chromatography-mass spectrometry (LC-MS) (Figure S4, Supporting Information). Based on the total net charges, we named each fluorophore as Tz-3, Tz-1, Tz+1, and Tz+3 (Figure 1b). The maximum absorption and emission wavelengths are in the NIR window (Figure S5, Supporting Information), where the combined absorption of NIR light and water/hemoglobin is minimal in addition to low autofluorescence.^[14] Physicochemical properties were calculated based on the final chemical structure using MarvinSketch 6.1.4 (ChemAxon), and optical properties were measured by using spectrophotometers (Ocean Optics). As shown in Figure 1c, logD values of Tz-fluorophores

increase in the order of Tz+3 < Tz-3 < Tz+1 < Tz-1, representing their lipophilicity under physiological conditions. However, both TPSA and HBA values showed a different trend for Tz+3 < Tz+1 = Tz-1 < Tz-3 because the sulfonate group has a high electron density and multiple sites for hydrogen bonding. Acidic pKa values represent that sulfonates are deprotonated under the physiological condition. The maximum excitation and emission wavelengths of all 4 Tz-fluorophores were similar in the NIR window. However, the introduction of different surface charges resulted in varying extinction coefficients and quantum yields due to the altered resonance of electrons in the pentamethine core (Figure 1c). To minimize the difference in molecular brightness, we adjusted the imaging exposure time for individual images based on the brightness obtained from in vitro and in vivo studies.

To validate the click efficiency in vitro, we treated B16F10 murine melanoma cells with TCO-PEG₄-NHS resulting in TCO-modified cells by conjugating NHS esters to the amines of proteins on the cell surface.^[15] Then, we treated each Tz-fluorophore to those TCO-modified cells at a concentration of 2×10^{-6} M in growth media. After 10 min incubation at 37 °C, all Tz-fluorophores exhibited over 15-fold higher fluorescence signals in TCO-modified cells compared with control cells where no TCO groups exist on the cell surface (Figure 2a).^[16] Although surface charges and lipophilicity cause immediate serum protein binding in cellular media and in the body,

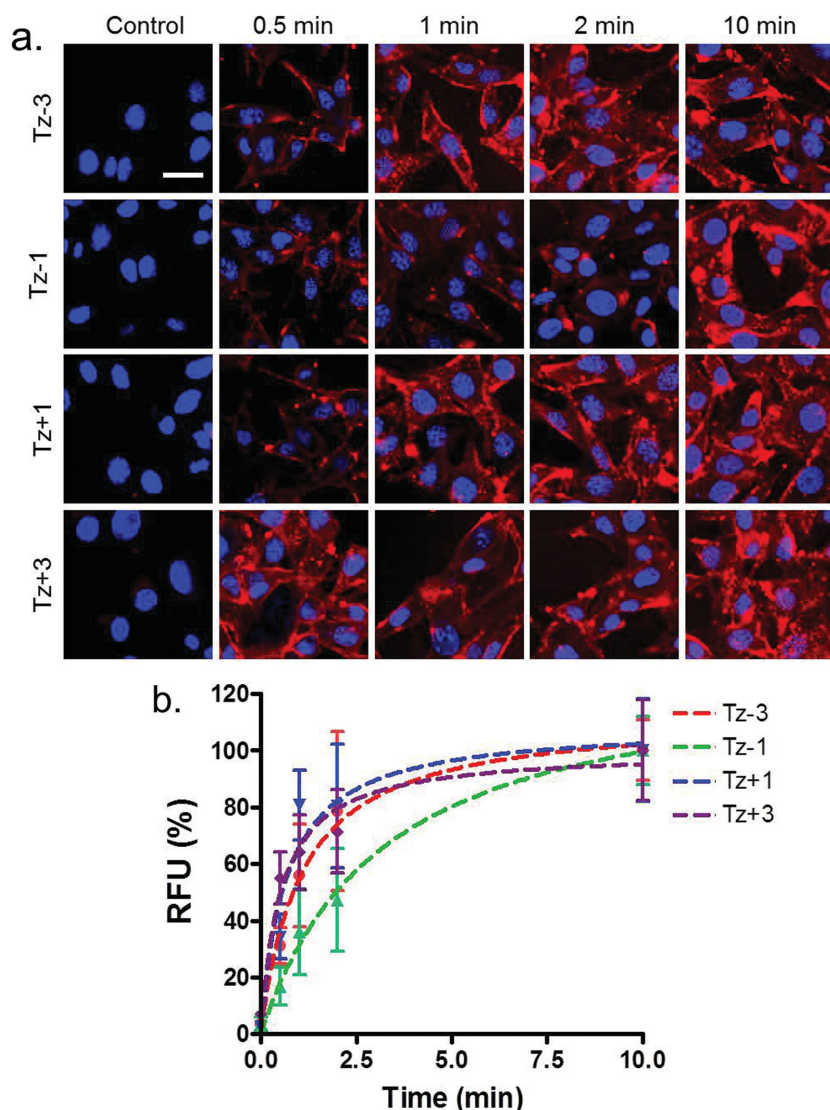


Figure 2. Click reaction between Tz-fluorophores and TCO-modified cells in vitro. a) Confocal images of TCO-modified B16F10 cells post-incubation of Tz-fluorophores. Blue = DAPI; red = 700 nm NIR fluorescence; scale bar = 10 μ m. b) Kinetics of bioorthogonal Tz-TCO click reactions ($n = 5$). Relative fluorescence intensity (RFU) was normalized by the maximum signal at 10 min post-incubation.

positively charged Tz+3 showed the fastest click reaction due to the thermodynamically favorable interactions between the cationic charges of Tz+3 and negatively charged cell surface. On the other hand, Tz-1 representing high lipophilicity ($\log D$ at pH 7.4 = 3.0) exhibited a relatively slow Tz-TCO reaction due to the low reaction concentration of fluorophores resulted from microaggregation. Tz-1, however, reached its steady state (V_{\max}) similar to the others at 10 min post-incubation, which represents the highly efficient click reactivity of Tz-fluorophores against TCO groups (Figure 2b). Interestingly, the reaction rate of Tz-1 was enhanced in serum-free media because of enriched binding of ligands to the cell surface without serum protein competition (Figure S6, Supporting Information).

Then, we evaluated how the altered chemical structure of fluorophores affects the pharmacokinetics, blood circulation,

and biodistribution in vivo. 10 nmol of each fluorophore was injected intravenously into C57BL/6J mice while exposing abdominal wall and major organs under the surgical field, and the biodistribution and clearance of each fluorophore were observed by an intraoperative imaging system^[10] for 4 h while collecting blood samples using capillary tubes (Figure 3a). Given the pharmacokinetics of Tz-fluorophores, all molecules distributed rapidly in the bloodstream, but cleared differently from the major organs. As shown in Figure 3b, the distribution half-life ($t_{1/2\alpha}$) of Tz-3 and Tz+3 was about 3–4-fold longer than that of Tz-1 and Tz+1. It shows that blood circulation is closely related to the physicochemical properties of each injected fluorophore, especially the surface charge and $\log D$ values as described in Figure 1.^[17,18] The terminal half-life ($t_{1/2\beta}$) of Tz-fluorophores followed a slightly different trend, showing a wide range of values depending on the lipophilicity. Interestingly, the $t_{1/2\beta}$ of Tz-1 is about 10-fold longer than the others, mainly because the lipophilic character promotes spontaneous binding to serum proteins, which drives the dye-protein complex mostly into the hepatobiliary clearance route (Figure 3c and Figure S7, Supporting Information).^[17] The rest of Tz-fluorophores followed both renal and hepatobiliary excretion as depicted in the biodistribution and clearance data observed by real-time intraoperative fluorescence imaging (Figure S7, Supporting Information). The other physiological and pharmacokinetic factors such as the area under the plasma concentration-time curve (AUC), volume of distribution (V_d), and plasma clearance were dependent on blood half-life values, although their extravasation rates are considered to be similar.^[19] However, the enhanced AUC and V_d of Tz-1 were resulted from the high $\log D$ value (3.0 at

pH 7.4), which contributed to tissue penetration, especially to the liver. The $\log D$ values of Tz-3 and Tz+3 are similar (–2.7 vs –3.2 at pH 7.4) and thus showed similar biodistribution, while Tz+3 with cationic charges required a longer elimination time compared to Tz-3 due to the delayed secretion caused by nonspecific ionic adhesion to the negatively charged cell surface.^[20]

We observed a similar trend in the resected tissues from the mice sacrificed at 4 h post-injection of Tz-fluorophores, which was quantified by the SBR of each major organ against surrounding muscle tissue (Figure 3d and Figure S8, Supporting Information). Tz-1 accumulated in liver and duodenum resulting in slow elimination from the body, while the rest of molecules majorly excreted by the kidneys and exhibited relatively fast excretion into bladder.

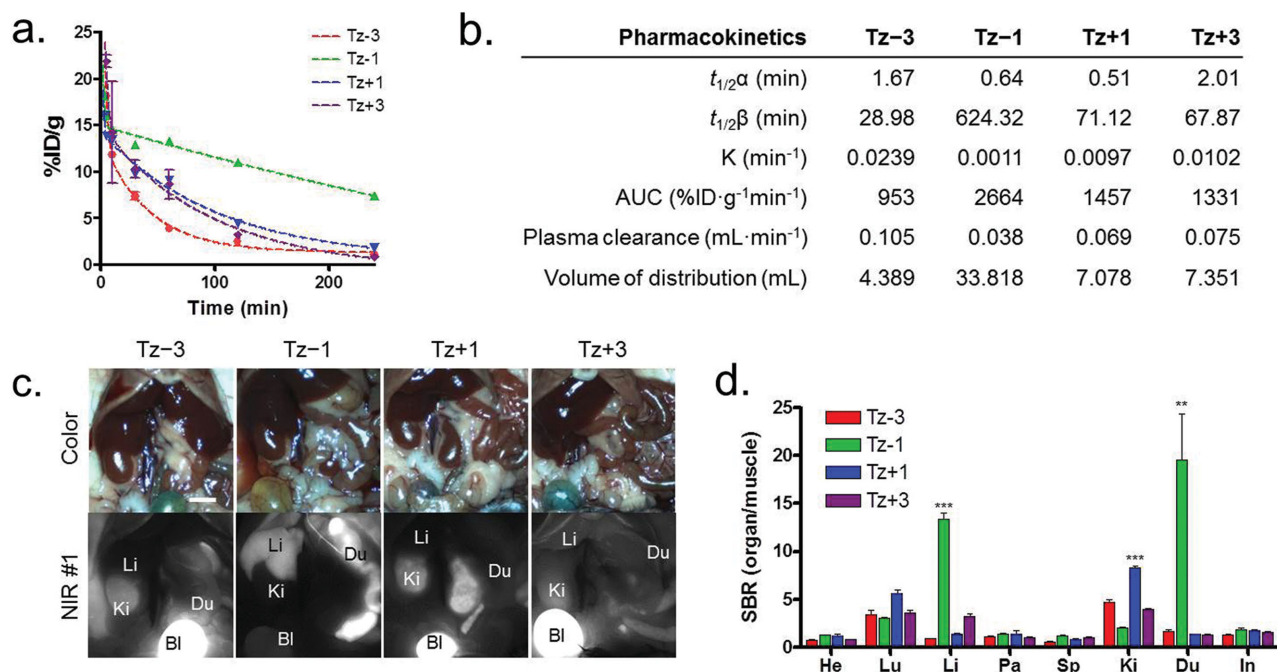


Figure 3. Pharmacokinetics and biodistribution of Tz-fluorophores in C57BL/6J mice: a,b) Time–concentration curves (a) and pharmacokinetic parameters (b) in blood. c,d) Intraoperative fluorescence images (c) and biodistribution (d) at 4 h post-injection (NIR #1:700 nm). Abbreviations used are: Bl, bladder; Du, duodenum; He, heart; In, intestine; Ki, kidneys; Li, liver; Lu, lungs; Pa, pancreas; Sp, spleen. Scale bar = 1 cm. ($n = 3$, mean \pm s.d., $**P < 0.01$, and $***P < 0.001$).

Finally, we determined the effect of the physicochemical properties and pharmacokinetics on the efficiency of click chemistry *in vivo*. We prepared TCO-modified B16F10 cells as described above and administered into syngeneic C57BL/6J mice intravenously to deposit them in lung capillaries, as previously reported.^[21] After 30 min, we injected each Tz-fluorophore to those TCO-presenting mice intravenously. After 4 h post-injection of Tz-fluorophores, animals were sacrificed and lung tissue was harvested to analyze the efficiency of *in vivo* click reaction by comparing fluorescence signals at 700 nm (NIR #1). Since cells were pre-labeled with an 800 nm emitting lipophilic fluorophore CTNF126 (NIR #2), the signals from Tz-fluorophores could be normalized based on the 800 nm emitting cell signals to minimize the potential errors resulting from different cell numbers deposited in the lung. Notably, Tz-fluorophores represented significantly higher signals in the lungs of TCO presenting mice compared to control mice administered with bare cells treated without TCO groups (Figure 4a).

The SBR of Tz-1 and Tz+1 were relatively low (1.42 and 1.09, respectively), which represents less efficient *in vivo* click chemistry (Figure 4b). This could be because of short $t_{1/2\alpha}$ and insufficient contact time of Tz-1 and Tz+1 fluorophores with the TCO-modified cells in lungs, resulted from rapid nonspecific uptake into liver (Tz-1) and kidneys (Tz+1) during the systemic circulation. In contrast, highly hydrophilic Tz-3 and Tz+3 exhibited high SBR (2.53 and 4.24, respectively) in the lung, representing favorably enhanced click reactions *in vivo*. These results emphasize the importance of defining the distribution half-life as a critical pharmacokinetic parameter, which reflects

the amount of Tz-fluorophores reaching the target cells in a reliable manner (Figure 4c).

In addition, the reduced lipophilicity and longer circulation contributed significantly to the molecular interactions *in vivo* as reported previously.^[18,22] Thus, we proved that the small molecule click moieties with optimized molecular properties could enhance bioorthogonal chemistry *in vivo* without using a large carrier (i.e., polymers or nanoparticles). Interestingly, Tz+3 outperformed Tz-3 with >50% higher click reactivity *in vivo*, while exhibiting only 20% longer distribution half-life. This is conceivably because the multiple positive surface charges have a profound effect on cellular accessibility in the luminal and interstitial spaces, which increase the chances for bioorthogonal click reaction *in vivo*.^[23] This result is in accordance with the previous report by Dearling and Packard where Cu-chelators with different surface charges changed their biodistribution significantly.^[24]

The reaction rate between the two chemicals, especially in the intravenous injection, is important because the contact time is limited by blood flow and/or active secretion processes in the body. The reaction rate constant of original azide-alkyne click chemistry has been reported to be about 10–100 M⁻¹ s⁻¹ (k_{obs}) per 10–100 $\times 10^{-6}$ M Cu(I) catalyst (Table 1).^[25] Strained alkynes without copper showed about 1000-fold slower click reaction (1–140 $\times 10^{-3}$ M⁻¹ s⁻¹),^[26] while the Tz-TCO reaction has been reported as fast as 6 $\times 10^3$ M⁻¹ s⁻¹,^[27] which is one of the fastest copper-free click reactions reported in literature. However, considering the association rate constant of biological ligands to their receptors (e.g., Nimotuzumab and epidermal growth

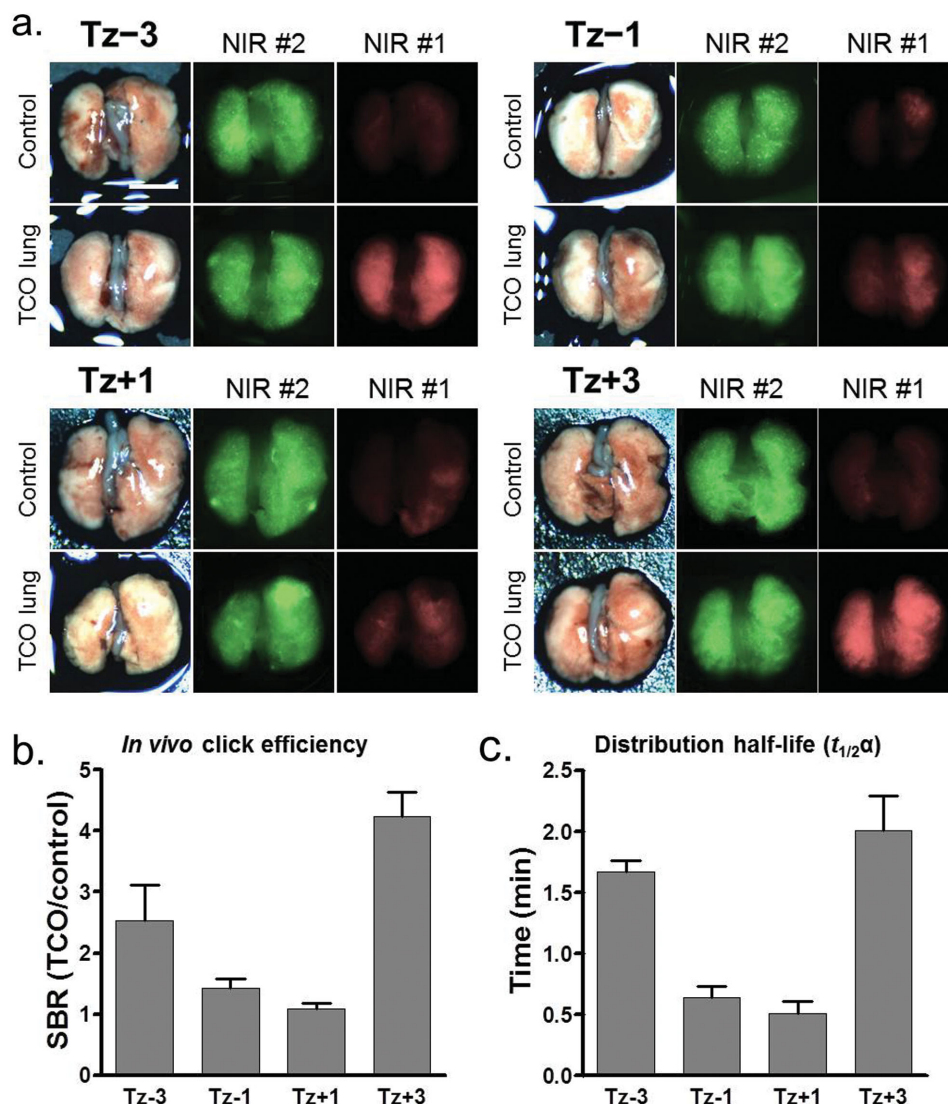


Figure 4. In vivo click chemistry of Tz-fluorophores against TCO-modified cells loaded in lungs. a) Ex vivo images of lung tissue excised 4 h post-injection of Tz-fluorophores (NIR #1: 700 nm and NIR #2: 800 nm). Scale bar = 1 cm. b,c) Distribution half-life (b) and in vivo click efficiency (c) of Tz-fluorophores. SBR represents the fluorescence signal from the lung tissue injected with TCO-modified cells divided by the signal from control cell-injected lung tissue without TCO.

factor receptor, $k_{on} = 5.2 \times 10^4 \text{ M}^{-1} \text{ s}^{-1}$),^[28] click chemistry is still slower than other biological binding processes.

Therefore, the longer circulation time of click moieties is particularly important to enhance the efficiency of in vivo click reactions. In addition, the combination of cationic charges and low logD (non-lipophilicity) of intravenously injected ligands played the critical role to improve surface click chemistry. However, it should be noted that other target models and biological

ligands could be dependent on the correlative response to the distribution half-life, where the click moieties need to be re-optimized to fit into the particular model system. For instance, zwitterionic or anionic charged small molecules show relatively short terminal half-life values and high volume of distribution due to the limited tissue penetration, which might be better candidates for peripheral tissue targets with considering other physiological and pharmacokinetic factors preferentially.

Table 1. Reaction kinetics for typical click chemistry.

Click reaction	Functional groups	2nd order rate constants ($\text{M}^{-1} \text{ s}^{-1}$)	Reference
Copper-catalyzed azide-alkyne cycloaddition	Alkyne, azide with copper catalyst	10–100 per $10^{-100} \times 10^{-6} \text{ M}$ Cu(I) catalyst	[25]
Strain-promoted azide-alkyne cycloaddition	Strained alkyne, azide	$1\text{--}140 \times 10^{-3}$	[26]
Inverse-demand Diels-Alder reaction	<i>Trans</i> -cyclooctene (TCO), tetrazine (Tz)	6×10^3	[27]

3. Conclusion

In summary, we have identified that surface charges and lipophilicity of injected molecules play the key role to achieve high reaction efficiency in bioorthogonal click chemistry. Despite the differences in physicochemical properties, all 4 Tz-fluorophores offered preferentially fast click reactions with TCO-modified cells in vitro within 10 min in biological media. However, their pharmacokinetics and biodistribution in animals were dependent upon the chemical structure, which governed the final click efficiency in vivo. These newly developed Tz-fluorophores can be used to label various biomaterials including nucleotide, protein, cells, and nanoparticles to control site-specific click reaction. Considering the applicability of copper-free click chemistry, the rationally designed chemical structures to control pharmacokinetics and biodistribution will lay the foundation of new-targeted contrast agents for optical, magnetic resonance, and nuclear imaging.

4. Experimental Section

Synthesis and Characterization of Tz-Fluorophore: Tz-amine ((4-(1,2,4,5-tetrazin-3-yl)phenyl)methanamine hydrochloride) was purchased from Sigma-Aldrich (St. Louis, MO). TCO-PEG₄-NHS (trans-cyclooctene-polyethylene glycol₄-N-hydroxysuccinimide ester) was purchased from Clickchemistrytools (Scottsdale, AZ). All other chemicals were purchased from Fisher Scientific (Pittsburgh, PA), Sigma-Aldrich (Saint Louis, MO) or Acros Organics (Morris Plains, NJ). Pentamethine fluorophores with assorted side groups were synthesized first, and they were conjugated with Tz-amine. Briefly, indols and bromides with different side groups were conjugated each other, and they were conjugated with Vilsmeier-Haack reagent to form pentamethine core. Then, 4-(2-carboxyethyl)phenylboronic acid were also conjugated to the intermediate to obtain additional acid group for further modification. Finally, the compounds were conjugated with Tz-amine through the conventional NHS chemistry. See Supporting Information for detailed chemical syntheses and analysis.

In Vitro Binding Assay of Tz-Fluorophores to TCO-Modified Cells: B16F10 murine melanoma cells were purchased from ATCC (Manassas, VA). Cells were maintained in DMEM (Gibco, Grand Island, NY), supplemented with 10% fetal bovine serum (FBS; Gibco), 100 U mL⁻¹ penicillin and 100 µg mL⁻¹ streptomycin (Gibco) at 37 °C in a humidified 5% CO₂ atmosphere. B16F10 cells were seeded onto four-chamber glass bottom dish at a density of 1 × 10⁵ cells per chamber in 1 mL full growth media. After overnight incubation, they were incubated with TCO-PEG₄-NHS (20 × 10⁻⁶ M in 1 mL PBS containing Ca²⁺ and Mg²⁺) for 30 min, followed by washing with PBS (pH 7.4) twice, they were further incubated with Tz-fluorophores (2 × 10⁻⁶ M in 1 mL full growth media) and Hoechst 33342 (Invitrogen, Carlsbad, CA) for varied time periods. Cellular images were obtained using a FV1000 multi-photon confocal microscope (Olympus, Tokyo, Japan) equipped with Laser Diode (405 and 633 nm) after washing and fixation with 2% formaldehyde solution for 5 min.

In Vivo Biodistribution and Pharmacokinetics of Tz-Fluorophores: Animals were housed in an AAALAC-certified facility and were studied under the supervision of BIDMC IACUC in accordance with the approved institutional protocol (#057-2014). Six weeks old C57BL/6 mice (male; 20–25 g) were purchased from Charles River Laboratories (Wilmington, MA). Animals were anesthetized with 100 mg kg⁻¹ ketamine and 10 mg kg⁻¹ xylazine intraperitoneally (Webster Veterinary, Fort Devens, MA). 10 nmol of the Tz-fluorophores in saline were administered intravenously, and animals were imaged using the real-time intraoperative dual-NIR channel imaging system.^[10] Herein, 670 nm excitation light (1 mW cm⁻²) and 760 nm excitation light (4 mW cm⁻²) were used with

white light (400–650 nm) at 40 000 lux. Color and NIR fluorescence images were acquired simultaneously with custom software at rates of up to 15 Hz over a field of view with a diameter of 15 cm. For each experiment, camera exposure time and image normalization was held constant. To quantify the distribution ($t_{1/2\alpha}$) and elimination ($t_{1/2\beta}$) blood half-life values, intermittent sampling from the tail vein was performed over the 4 h period following a single intravenous administration. Approximately 10–20 µL of blood were collected using glass capillary tubes at the following time points: 0, 3, 5, 10, 30, 60, 120, and 240 min. The same intraoperative imaging system was used to measure the fluorescence intensity of each sample, and the concentration was calculated based on the image SBR using a standard curve for each fluorophore. Animals were injected with Tz-fluorophores 4 h prior to imaging, and major organs were resected, imaged, and the signal from each organ/tissue was quantified by measuring fluorescent intensity (photons s⁻¹ cm⁻² sr⁻¹). At least three animals were analyzed at each time point. Results were presented as mean ± s.d. and curve fitting was performed using Prism version 4.0a software (GraphPad, San Diego, CA).

In Vivo Click Chemistry between Tz-Fluorophores and TCO-Modified Cells: TCO-modified B16F10 cells were prepared as above and stained with an 800 nm emitting lipophilic cation CTNF126 for 30 min incubation. After detachment of labeled cells with cell scraper, the TCO-modified cells (1 × 10⁶ cells per mouse) were injected intravenously into C57BL/6 mice. 10 nmol of each Tz-fluorophore in saline were administered intravenously into the same mice 30 min post-injection of cells. Animals were sacrificed 4 h post-injection of Tz-fluorophores, and lungs were resected, imaged, and analyzed by using the custom-built imaging system.

Quantitative Analysis: The fluorescence and background intensity of a region of interest over each tissue was quantified using custom imaging software and ImageJ v1.48 (NIH, Bethesda, MD). The SBR was calculated as SBR = fluorescence/background, where background is the signal intensity of muscle. All NIR fluorescence images for a particular Tz-fluorophore were normalized identically for all conditions of an experiment. A one-way ANOVA followed by Tukey's multiple comparisons test were used to assess the statistical differences between multiple groups. A *P*-value of less than 0.05 was considered significant: **P* < 0.05, ***P* < 0.01, and ****P* < 0.001. Results are presented as mean ± standard deviation (s.d.).

Supporting Information

Supporting Information is available from the Wiley Online Library or from the author.

Acknowledgements

H.K. and J.H.L. contributed equally to this work. This study was supported by the following grants from NIH: NIBIB #R01-EB-011523 (H.S.C.) and #R01-EB017699 (H.S.C.), NCI #R01-CA-192878 (S.H.Y.), and the Basic Science Research Program through the National Research Foundation of Korea (NRF) funded by the Ministry of Education (2016R1C1B3013951) (H.K.).

Received: May 30, 2016

Revised: July 11, 2016

Published online: August 29, 2016

- [1] M. Boyce, C. R. Bertozzi, *Nat. Meth.* **2011**, *8*, 638.
- [2] S. T. Laughlin, J. M. Baskin, S. L. Amacher, C. R. Bertozzi, *Science* **2008**, *320*, 664.
- [3] F. Emmetiere, C. Irwin, N. T. Viola-Villegas, V. Longo, S. M. Cheal, P. Zanzonico, N. Pillarsetty, W. A. Weber, J. S. Lewis, T. Reiner, *Bioconj. Chem.* **2013**, *24*, 1784.

- [4] R. Rossin, P. R. Verkerk, S. M. van den Bosch, R. C. M. Vuldens, I. Verel, J. Lub, M. S. Robillard, *Angew. Chem. Int. Ed.* **2010**, *49*, 3375.
- [5] A. Zlitni, N. Janzen, F. S. Foster, J. F. Valliant, *Angew. Chem. Int. Ed.* **2014**, *53*, 6459.
- [6] H. Koo, S. Lee, J. H. Na, S. H. Kim, S. K. Hahn, K. Choi, I. C. Kwon, S. Y. Jeong, K. Kim, *Angew. Chem. Int. Ed.* **2012**, *51*, 11836.
- [7] N. K. Devaraj, G. M. Thurber, E. J. Keliher, B. Marinelli, R. Weissleder, *Proc. Natl. Acad. Sci. USA* **2012**, *109*, 4762.
- [8] K. Petrak, P. Goddard, *Adv. Drug. Del. Rev.* **1989**, *3*, 191.
- [9] A. Elsaesser, C. V. Howard, *Adv. Drug Del. Rev.* **2012**, *64*, 129.
- [10] H. Hyun, M. H. Park, E. A. Owens, H. Wada, M. Henary, H. J. M. Handgraaf, A. L. Vahrmeijer, J. V. Frangioni, H. S. Choi, *Nat. Med.* **2015**, *21*, 192.
- [11] H. Hyun, H. Wada, K. Bao, J. Gravier, Y. Yadav, M. Laramie, M. Henary, J. V. Frangioni, H. S. Choi, *Angew. Chem. Int. Ed.* **2014**, *53*, 10668.
- [12] H. Hyun, E. A. Owens, H. Wada, A. Levitz, G. Park, M. H. Park, J. V. Frangioni, M. Henary, H. S. Choi, *Angew. Chem. Int. Ed.* **2015**, *54*, 8648.
- [13] H. S. Choi, S. L. Gibbs, J. H. Lee, S. H. Kim, Y. Ashitate, F. Liu, H. Hyun, G. Park, Y. Xie, S. Bae, M. Henary, J. V. Frangioni, *Nat. Biotechnol.* **2013**, *31*, 148.
- [14] R. Weissleder, *Nat. Biotechnol.* **2001**, *19*, 316.
- [15] R. Selvaraj, J. M. Fox, *Curr. Opin. Chem. Biol.* **2013**, *17*, 753.
- [16] N. K. Devaraj, R. Weissleder, *Acc. Chem. Res.* **2011**, *44*, 816.
- [17] H. S. Choi, W. Liu, P. Misra, E. Tanaka, J. P. Zimmer, B. Itty Ipe, M. G. Bawendi, J. V. Frangioni, *Nat. Biotechnol.* **2007**, *25*, 1165.
- [18] H. S. Choi, K. Nasr, S. Alyabyev, D. Feith, J. H. Lee, S. H. Kim, Y. Ashitate, H. Hyun, G. Patonay, L. Strekowski, M. Henary, J. V. Frangioni, *Angew. Chem. Int. Ed.* **2011**, *50*, 6258.
- [19] R. L. Dedrick, M. F. Flessner, *J. Natl. Cancer Inst.* **1997**, *89*, 480.
- [20] H. Lodish, A. Berk, S. L. Zipursky, P. Matsudaira, D. Baltimore, J. Darnell, *Molecular Cell Biology*, W. H. Freeman, New York, USA **2000**.
- [21] T. Maldiney, A. Bessière, J. Seguin, E. Teston, S. K. Sharma, B. Viana, A. J. J. Bos, P. Dorenbos, M. Bessodes, D. Gourier, D. Scherman, C. Richard, *Nat. Mater.* **2014**, *13*, 418.
- [22] R. P. Lyon, T. D. Bovee, S. O. Doronina, P. J. Burke, J. H. Hunter, H. D. Neff-LaFord, M. Jonas, M. E. Anderson, J. R. Setter, P. D. Senter, *Nat. Biotechnol.* **2015**, *33*, 733.
- [23] S. Rounds, C. A. Vaccaro, *Am. Rev. Respir. Dis.* **1987**, *135*, 725.
- [24] J. L. J. Dearling, B. M. Paterson, V. Akurathi, S. Betanzos-Lara, S. T. Treves, S. D. Voss, J. M. White, J. S. Huston, S. V. Smith, P. S. Donnelly, A. B. Packard, *Bioconj. Chem.* **2015**, *26*, 707.
- [25] S. V. Orski, G. R. Sheppard, S. Arumugam, R. M. Arnold, V. V. Popik, J. Locklin, *Langmuir* **2012**, *28*, 14693.
- [26] M. F. Debets, S. S. van Berkel, J. Dommerholt, A. J. Dirks, F. P. J. T. Rutjes, F. L. van Delft, *Acc. Chem. Res.* **2011**, *44*, 805.
- [27] N. K. Devaraj, R. Upadhyay, J. B. Haun, S. A. Hilderbrand, R. Weissleder, *Angew. Chem. Int. Ed.* **2009**, *48*, 7013.
- [28] A. Talavera, R. Friemann, S. Gómez-Puerta, C. Martínez-Fleites, G. Garrido, A. Rabasa, A. López-Requena, A. Pupo, R. F. Johansen, O. Sánchez, U. Krengel, E. Moreno, *Cancer Res.* **2009**, *69*, 5851.



Supporting Information

for *Adv. Healthcare Mater.*, DOI: 10.1002/adhm.201600574

Site-Specific In Vivo Bioorthogonal Ligation via Chemical Modulation

Heebeom Koo, Jeong Heon Lee, Kai Bao, Yunshan Wu, Georges El Fakhri, Maged Henary, Seok Hyun Yun,* and Hak Soo Choi**

Supporting information

Site-specific *in vivo* bioorthogonal ligation *via* chemical modulation

Heebeom Koo,^{1,4,*} Jeong Heon Lee,^{2,5,*} Kai Bao,² Yunshan Wu,³ Georges El Fakhri,⁵
Maged Henary,^{3,**} Seok Hyun Yun,^{1,**} and Hak Soo Choi^{2,5,**}

* These authors contributed equally

¹ Wellman Center for Photomedicine, Massachusetts General Hospital and Harvard Medical School, Cambridge, MA 02139

² Division of Hematology/Oncology, Department of Medicine, Beth Israel Deaconess Medical Center and Harvard Medical School, Boston, MA 02215

³ Department of Chemistry, Center for Diagnostics and Therapeutics, Georgia State University, Atlanta, GA 30303

⁴ Department of Medical Lifescience, College of Medicine, The Catholic University of Korea, Seoul 137-701, South Korea

⁵ Gordon Center for Medical Imaging, Department of Radiology, Massachusetts General Hospital and Harvard Medical School, Boston, MA 02114

** Correspondence to: mhenary1@gsu.edu, syun@hms.harvard.edu or hchoi12@mgh.harvard.edu

The PDF file includes:

Supplementary Methods

Figure S1. General synthesis for various pentamethine carbocyanine dyes.

Figure S2. Synthesis for Tz-fluorophores by conjugating pentamethines with Tz-amine.

Figure S3. Chemical structures of Tz-fluorophores and their molecular properties.

Figure S4. HPLC data for Tz-fluorophores.

Figure S5. Optical properties of Tz-fluorophores.

Figure S6. Binding of Tz-1 with TCO-modified cells in serum-free culture media.

Figure S7. Real-time *in vivo* fluorescence images of Tz-fluorophore-injected mice.

Figure S8. *Ex vivo* fluorescence images of resected organs from Tz-fluorophore-injected mice.

Supplementary Methods

Materials: All chemicals and solvents were of American Chemical Society grade or HPLC purity and were used as received. HPLC grade acetonitrile (CH₃CN) and water were purchased from VWR International (West Chester, PA) and American Bioanalytic (Natick, MA), respectively. Tz-amine ((4-(1,2,4,5-tetrazin-3-yl)phenyl)methanamine hydrochloride) was purchased from Sigma-Aldrich (St. Louis, MO). TCO-PEG₄-NHS (*trans*-cyclooctene-polyethylene glycol₄-*N*-hydroxysuccinimide ester) was purchased from Click chemistry tools (Scottsdale, AZ). All other chemicals were purchased from Fisher Scientific (Pittsburgh, PA), Sigma-Aldrich and Acros Organics.

The reactions were followed using silica gel 60 F₂₅₄ thin layer chromatography plates (Merck EMD Millipore, Darmstadt, Germany). Open column chromatography was utilized for the purification of all hydrophobic final compounds using 60-200 μm, 60Å classic column silica gel (Dynamic Adsorbents, Norcross, GA). Highly charged final products were isolated using reversed phase C18 column chromatography (Fluka). ¹H NMR spectra were obtained using high quality Kontes NMR tubes (Kimble Chase, Vineland, NJ) rated to 500 MHz and were recorded on a Bruker Avance (400 MHz) spectrometer using D₂O or DMSO-*d*₆ containing tetramethylsilane (TMS) as an internal calibration standard set to 0.0 ppm. NMR abbreviations used throughout the experimental section are as follows, s = singlet, d = doublet, t = triplet, q = quartet, p = pentet, m = multiplet, dd = doublet doublets, and bs = broad singlet. UV-Vis/NIR absorption spectra were recorded on a Varian Cary 50 spectrophotometer. High-resolution accurate mass spectra (HRMS) were obtained either at the GSU Mass Spectrometry Facility using a Waters Q-TOF micro (ESI-Q-TOF) mass spectrometer or utilizing a Waters Micromass LCT TOF ES+ Premier Mass Spectrometer. The purity of each compound tested was determined by using LC/MS instrument possessing a Waters 2487 single wavelength absorption detector with wavelengths set between 640 and 700 nm depending on the particular photophysical properties. The column used in LC was a Waters Delta-Pak 5 μM 100Å 3.9×150 mm reversed phase C₁₈ column, with a flow rate of 1mL/min employing a 5-100% acetonitrile/water/0.1% formic acid gradient; a SEDEX 75 Evaporative light scattering detection (ELSD) was also utilized in tandem with liquid chromatography to confirm purity. All compounds tested were > 95% pure.

Synthesis and characterization of pentamethine cyanine dyes: The pentamethine carbocyanine dyes functionalized with a bromine atom at the meso carbon **3**, **4**, **9** and **10** were synthesized according to our published procedures [1-4]. The final Tz-fluorophores were dissolved in water and purified by a Waters preparative HPLC system (Milford, MA) using acetonitrile (ACN) and water including 0.1% trifluoroacetic acid (TFA). The synthesis of final compounds **5**, **6**, **11** and **12**, and the Tz-fluorophore conjugates were outlined in Figures S1 and S2, respectively.

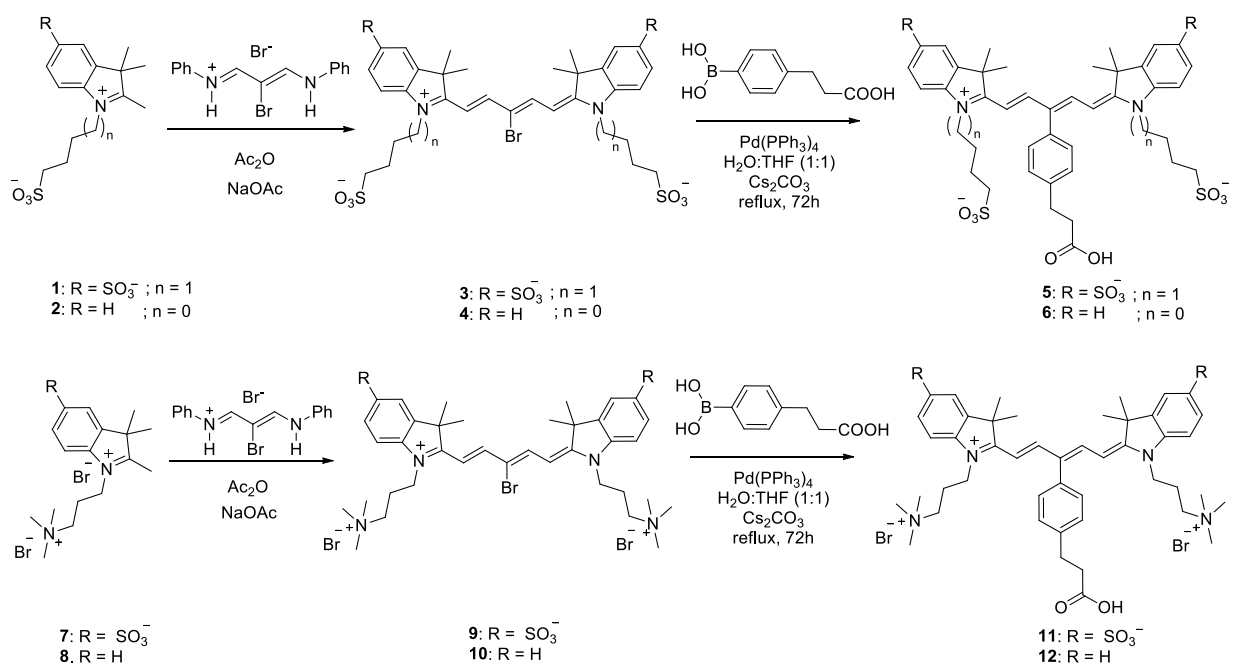
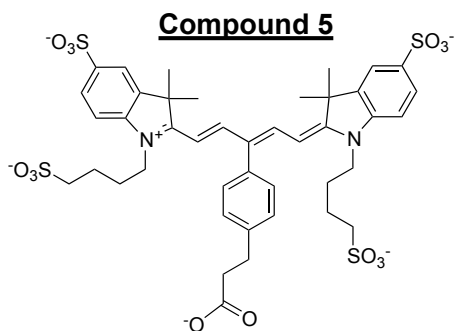


Figure S1. General synthesis for various pentamethine carbocyanine dyes **5**, **6**, **11** and **12**.

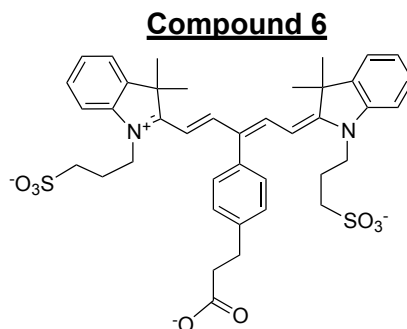
2-((1*E*,3*Z*,5*E*)-3-(4-(2-carboxyethyl)phenyl)-5-(3,3-dimethyl-5-sulfonato-1-(4-sulfonatobutyl)-indolin-2-ylidene)penta-1,3-dien-1-yl)-3,3-dimethyl-1-(4-sulfonatobutyl)-3*H*-indol-1-ium-5-sulfonate (Compound 5).



Chemical Formula: C₄₂H₄₆N₂O₁₄S₄⁴⁻
Exact Mass: 930.19

2-((1*E*,3*Z*,5*Z*)-3-bromo-5-(3,3-dimethyl-6-sulfonato-1-(4-sulfonatobutyl)indolin-2-ylidene) penta-1,3-dien-1-yl)-3,3-dimethyl-1-(4-sulfonatobutyl)-3*H*-indol-1-ium-6-sulfonate **3** (160 mg), 3-(4-boronophenyl)propanoic acid (60.8 mg) and cesium carbonate (30.2 mg) was stirred in water and to this solution was added tetrakis(triphenylphosphine)palladium (0) (10%). The reaction mixture was heated to reflux for 3 days. The mixture was cooled to room temperature and filtered then the filtrate was concentrated under reduced pressure to give a crude product as blue residue. The crude was loaded on a reverse phase column and eluent with MeOH in water to give the product **5**. Yield 34%; mp 285°C (decomposed). ¹H NMR (400 MHz, D₂O) 8.16 (d, *J* = 13.9 Hz, 2 H), 7.83 (s, 2 H), 7.75 (d, *J* = 8.1 Hz, 2 H), 7.49 (d, *J* = 7.1 Hz, 2 H), 7.14 (t, *J* = 7.6 Hz, 2 H), 5.71 (d, *J* = 13.9 Hz, 2 H), 3.64 (br. s., 4 H), 3.10 - 2.95 (m, 2 H), 2.74 (br. s., 6 H), 1.96 (s, 2 H), 1.66 (br. s., 12 H), 1.60 (br. s., 6 H). ¹³C NMR (100 MHz, D₂O) 174.0, 153.3, 143.8, 141.5, 139.1, 130.2, 129.2, 126.6, 119.7, 111.0, 102.6, 50.3, 49.0, 43.3, 30.6, 26.7, 25.5, 21.5. HRMS (TOF-MS ES⁻), calculated for C₄₂H₄₆N₂O₁₄S₄⁴⁻: *m/z* 930.1854 [M]⁻, found: *m/z* 930.1982 [M]⁻.

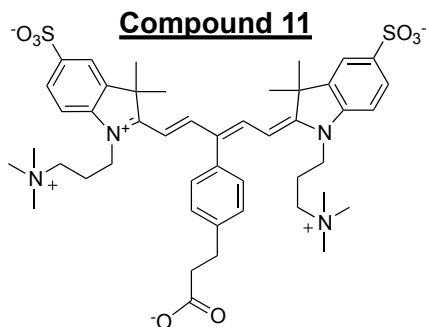
3-((*E*)-2-((2*Z*,4*E*)-3-(4-(2-carboxyethyl)phenyl)-5-(3,3-dimethyl-1-(3-sulfonatopropyl)-3*H*-indol-1-ium-2-yl) penta-2,4-dien-1-ylidene)-3,3-dimethylindolin-1-yl)propane-1-sulfonate (Compound 6).



Chemical Formula: $C_{40}H_{44}N_2O_8S_2^{2-}$
Exact Mass: 744.26

3-((*Z*)-2-((*Z*,*4E*)-3-bromo-5-(3,3-dimethyl-1-(3-sulfonatopropyl)-3*H*-indol-1-ium-2-yl)penta-2,4-dien-1-ylidene)-3,3-dimethylindolin-1-yl)propane-1-sulfonate **4** (200 mg), 3-(4-borono-phenyl)propanoic acid (103.2 mg) and cesium carbonate (48.15 mg) was stirred in water and THF (1:1) and to this solution was added tetrakis(triphenylphosphine)palladium (0) (10%). The reaction mixture was refluxed for 3 days and cooled to room temperature. The mixture was filtered and solvents were evaporated. The crude product was separated by reverse phase column chromatography to afford the pure final compound **6** (45 mg). Yield 25%; mp > 268°C. 1H NMR (400 MHz, DMSO- d_6) 8.53 (d, $J = 13.9$ Hz, 1 H), 7.98 (t, $J = 6.9$ Hz, 2 H), 7.83 (d, $J = 3.5$ Hz, 4 H), 7.77 (s, 1 H), 7.74 (br. s., 2 H), 7.69 (br. s., 1 H), 7.63 (d, $J = 7.6$ Hz, 2 H), 7.47 (d, $J = 7.8$ Hz, 3 H), 7.41 (t, $J = 7.6$ Hz, 2 H), 7.27 (t, $J = 7.3$ Hz, 2 H), 7.19 (d, $J = 7.8$ Hz, 1 H), 5.71 (d, $J = 14.1$ Hz, 2 H), 3.95 (br. s., 4 H), 3.06 - 2.90 (m, 3 H), 2.66 (t, $J = 7.1$ Hz, 4 H), 2.42 (br. s., 4 H), 1.89 (br. s., 4 H), 1.72 (br. s., 12 H). ^{13}C NMR (100 MHz, DMSO- d_6) 173.5, 173.4, 172.5, 142.2, 140.9, 140.4, 135.3, 134.6, 134.5, 130.5, 130.4, 129.9, 129.1, 128.4, 124.9, 122.5, 118.4, 117.5, 115.3, 111.2, 100.9, 49.1, 48.1, 43.0, 35.7, 34.1, 30.5, 30.2, 27.0, 23.2. HRMS (TOF-MS ES-), calculated for $C_{40}H_{44}N_2O_8S_2^{2-}$: m/z 744.2550 [M] $^-$, found: m/z 744.2684 [M] $^-$.

3-(4-((*1E*,*3Z*,*5E*)-1-(3,3-dimethyl-5-sulfonato-1-(3-(trimethylammonio)propyl)-3*H*-indol-1-ium-2-yl)-5-(3,3-dimethyl-5-sulfonato-1-(3-(trimethylammonio)propyl)indolin-2-ylidene)penta-1,3-dien-3-yl)phenyl)propanoate (Compound **11**).

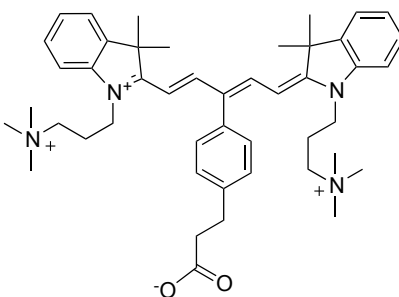


Chemical Formula: C₄₆H₆₀N₄O₈S₂
Exact Mass: 860.39

To a solution of the 2-((1*E*,3*Z*,5*E*)-3-bromo-5-(3,3-dimethyl-5-sulfonato-1-(3-(trimethylammonio)propyl)indolin-2-ylidene)penta-1,3-dien-1-yl)-3,3-dimethyl-1-(3-(trimethylammonio)propyl)-3*H*-indol-1-ium-5-sulfonate **9** (1.0 g, 1.15 mmol), 4-(2-carboxyethyl)phenylboronic acid (0.45 g, 2.32 mmol) and cesium carbonate (0.89 g, 2.73 mmol) in a mixture of EtOH (15 mL) and water (15 mL) under N₂ at room temperature, was added tetrakis(triphenyl phosphine)palladium (0) (99 mg, 0.09 mmol) and the reaction mixture was stirred at 60°C for 4 h while monitoring by Vis/NIR spectrophotometry. The mixture was filtered and solvents were evaporated. The crude product was separated by reverse phase column chromatography to afford the pure final compound **11** as a blue solid (0.67 g). Yield 78%; mp > 260°C; ¹H NMR (400 MHz, DMSO-*d*₆), δ: 12.33 (s, 1H), 8.54 (d, *J* = 7.0 Hz, 2H), 7.87 (s, 1H), 7.60 (d, *J* = 4.2 Hz, 2H), 7.42 (d, *J* = 4.0 Hz, 2H), 7.35 (d, *J* = 4.2 Hz, 2H), 7.27 (d, *J* = 3.8 Hz, 2H), 6.65 (d, *J* = 7.0 Hz, 2H), 3.84 (br s, 4H), 3.25 (br s, 4H), 3.08 (s, 18H), 2.93 (br s, 2H), 2.65 (br s, 2H), 1.99 (br s, 4H), 1.78 (s, 12H); ¹³C NMR (100 MHz, D₂O, 70°C), δ: 181.88, 175.21, 155.23, 143.57, 142.04, 141.23, 137.19, 133.25, 130.67, 129.92, 127.51, 120.49, 111.37, 102.87, 63.95, 53.84, 49.82, 41.30, 39.42, 32.25, 27.51, 21.16; HRMS (TOF-MS ES⁺), calculated for C₄₆H₆₀N₄O₈S₂: *m/z* 860.3853 [M]⁺, found: *m/z* 862.3946 [M+2H]⁺.

*3-(4-((1*E*,3*Z*)-1-(3,3-dimethyl-1-(3-(trimethylammonio)propyl)-3*H*-indol-1-ium-2-yl)-5-((*E*)-3,3-dimethyl-1-(3-(trimethylammonio)propyl)indolin-2-ylidene)penta-1,3-dien-3-yl)phenyl)-propanoate (Compound **12**).*

Compound 12



Chemical Formula: $C_{46}H_{62}N_4O_2^{2+}$
Exact Mass: 702.49

To a solution of 2-((1*E*,3*Z*)-3-bromo-5-((*E*)-3,3-dimethyl-1-(3-(trimethylammonio)propyl)indolin-2-ylidene)penta-1,3-dien-1-yl)-3,3-dimethyl-1-(3-(trimethylammonio)propyl)-3*H*-indol-1-ium **10** (1.15 mmol), 4-(2-carboxyethyl)phenylboronic acid (2.32 mmol) and cesium carbonate (3 mmol) in a mixture of EtOH (15 mL) and water (15 mL) under N_2 at room temperature, was added tetrakis(triphenyl phosphine)palladium (0) (0.1 mmol) and the reaction mixture was stirred at 60°C for 4 h while monitoring by Vis/NIR spectrophotometry and alumina TLC plates eluting with 1% methanol in dichloromethane. After the reaction was finished as indicated by the consumption of starting bromo compound, the solvent was evaporated under vacuum and the residue was purified by precipitation from methanol using diethyl ether. Several precipitations and washing with acetone, ether and ethyl acetate afforded the final purified compound **12** as a blue-green solid. Yield 57%; mp > 220°C. 1H NMR (400 MHz, D_2O), δ : 8.16 (d, $J = 14.0$ Hz, 2H), 7.51-7.15 (m, 12H), 5.75 (d, $J = 14.0$ Hz, 2H), 3.83 (br s, 4H), 3.21 (br s, 4H), 3.09 (br s, 2H), 2.97 (s, 18H), 2.77 (br s, 2H), 2.04 (br s, 4H), 1.67 (s, 12H). HRMS (TOF-MS ES+), calculated for $C_{46}H_{62}N_4O_2^{2+}$: m/z 702.4862 $[M]^+$, found: m/z 702.4854 $[M]^+$.

Synthesis and characterization of Tz-fluorophores: To activate the carboxylic acid of compound **5**, **6**, **11** or **12**, each compound was completely dissolved in anhydrous methyl sulfoxide and dipyrrolidino(*N*-succinimidyl)carbenium hexafluorophosphate (HSPyU 10.0 eq) was added with the presence of *N,N*-diisopropylethylamine (DIEA 2.5 eq). The reaction mixture was stirred at room temperature for 2 h, followed by adding the *N*-hydroxysuccinimide (NHS) ester form **5** into 10-fold anhydrous ethyl acetate for precipitation. The precipitated solid was washed with ethyl acetate and dried *in vacuo*. Then, compound **13** was dissolved in anhydrous dimethyl sulfoxide (DMSO), followed by addition of DIEA (2.5 eq) and Tz-amine (1.1 eq), respectively. The reaction mixtures were stirred at room temperature for 2 h. The final products were purified by a Waters preparative HPLC system using ACN and water including 0.1% TFA, and were obtained as a blue solid. The purity of Tz-fluorophores was confirmed by using a Waters LC/MS QDa system (Acquity, Milford, MA) equipped with a multi-wavelength fluorescence detector (FLD; Waters 2475), a photodiode array (PDA) detector (Waters 996), and a QDa mass detector (Waters Acquity).

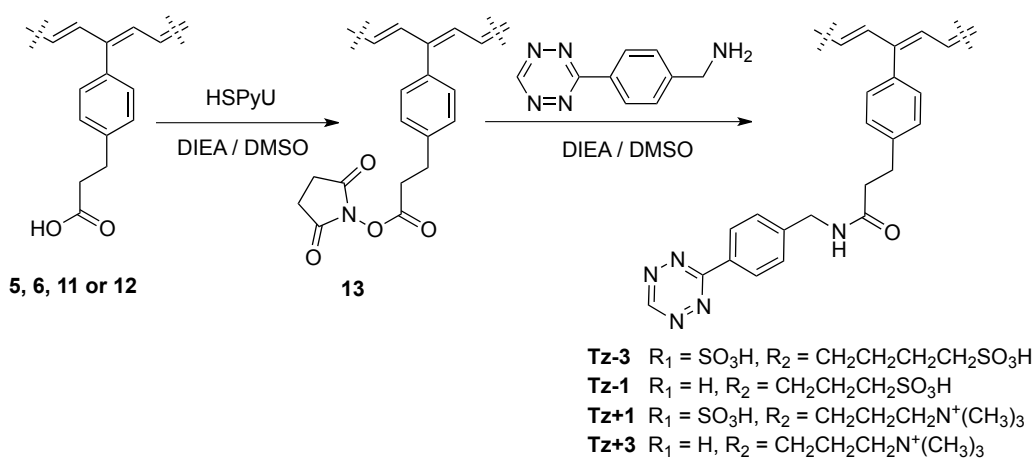


Figure S2. Synthesis for Tz-fluorophores by conjugating compound **5**, **6**, **11** or **12** with Tz-NH₂.

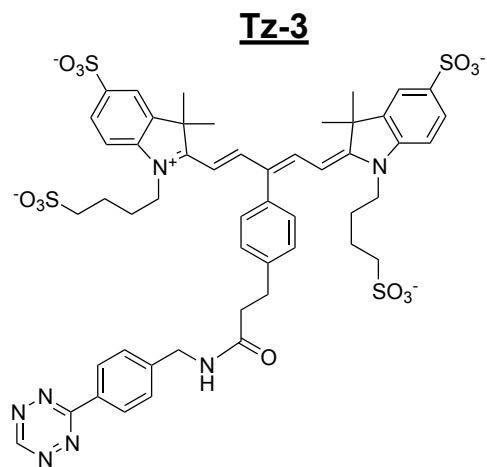
2-((1*E*,3*Z*,5*E*)-3-(4-(3-((4-(1,2,4,5-tetrazin-3-yl)benzyl)amino)-3-oxopropyl)phenyl)-5-(3,3-dimethyl-5-sulfonato-1-(4-sulfonatobutyl)indolin-2-ylidene)penta-1,3-dien-1-yl)-3,3-dimethyl-1-

(4-sulfonatobutyl)-3H-indol-1-ium-5-sulfonate (Tz-3): Column: ODS-AMQ anionic exchange column (YMC, particle size: 5.0 μm , length: 6.0 \times 150 mm), gradient (10 to 90 of B, A: water with 10 mM triethylammonium acetate (TEAA), B: MeOH with 10 mM TEAA), flow rate: 1 mL/min, running time: 15 min, sample amount: 5 nmol, pressure: up to 1400 psi. HPLC-MS (Quad MS ES⁻), calculated for C₅₁H₅₄N₇O₁₃S₄³⁻: m/z 1100.27 [M]⁻, found: m/z 550.81 [M]²⁻.

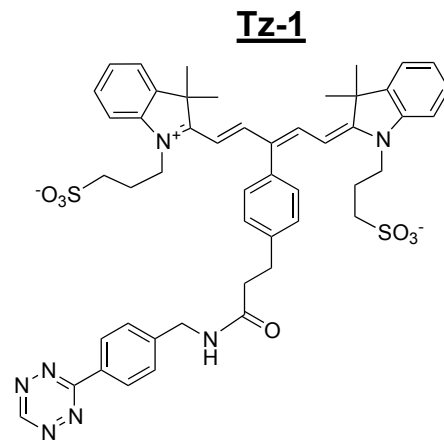
3-((E)-2-((2Z,4E)-3-(4-(3-((4-(1,2,4,5-tetrazin-3-yl)benzyl)amino)-3-oxopropyl)phenyl)-5-(3,3-dimethyl-1-(3-sulfonatopropyl)-3H-indol-1-ium-2-yl)penta-2,4-dien-1-ylidene)-3,3-dimethylindolin-1-yl)propane-1-sulfonate (Tz-1): Column: ODS-AMQ anionic exchange column (YMC, particle size: 5.0 μm , length: 6.0 \times 150 mm), gradient (10 to 90 of B, A: water with 10 mM TEAA, B: MeOH with 10 mM TEAA), flow rate: 1 mL/min, running time: 15 min, sample amount: 5 nmol, pressure: up to 1400 psi. HPLC-MS (Quad MS ES⁻), calculated for C₄₉H₅₂N₇O₇S₂⁻: m/z 914.34 [M]⁻, found: m/z 914.50 [M]⁻.

2-((1E,3Z,5E)-3-(4-(3-((4-(1,2,4,5-tetrazin-3-yl)benzyl)amino)-3-oxopropyl)phenyl)-5-(3,3-dimethyl-5-sulfonato-1-(3-(trimethylammonio)propyl)indolin-2-ylidene)penta-1,3-dien-1-yl)-3,3-dimethyl-1-(3-(trimethylammonio)propyl)-3H-indol-1-ium-5-sulfonate (Tz+1): Column: Ultra AQ C18 (Restek, particle size: 5.0 μm , length: 4.6 \times 150 mm), gradient (10 to 90 of B, A: water with 0.1% formic acid (FA), B: ACN with 0.1% FA), flow rate: 1 mL/min, running time: 30 min, sample amount: 5 nmol, pressure: up to 1400 psi. HPLC-MS (Quad MS ES⁺), calculated for C₅₅H₆₈N₉O₇S₂⁺: m/z 1030.47 [M]⁺, found: m/z 1030.79 [M]⁺.

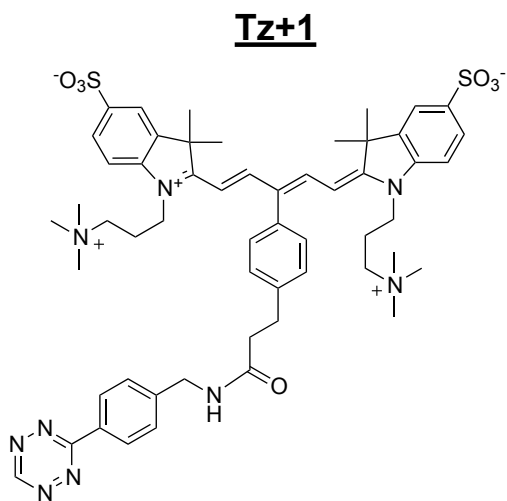
2-((1E,3Z,5E)-3-(4-(3-((4-(1,2,4,5-tetrazin-3-yl)benzyl)amino)-3-oxopropyl)phenyl)-5-(3,3-dimethyl-1-(3-(trimethylammonio)propyl)indolin-2-ylidene)penta-1,3-dien-1-yl)-3,3-dimethyl-1-(3-(trimethylammonio)propyl)-3H-indol-1-ium (Tz+3): Colum: Proshell 120, EC-C18 (Agilent, particle size: 2.7 μm , length: 3.0 \times 50 mm), gradient (10 to 90 of B, A: water with 0.1 M ammonium acetate, B: ACN with 0.1% FA), flow rate: 1 mL/min, running time: 15 min, sample amount: 5 nmol, pressure: up to 3300 psi. HPLC-MS (Quad MS ES⁺), calculated for C₅₅H₇₀N₉O³⁺: m/z 872.57 [M]⁺, found: m/z 465.97 [M+CH₃CO₂]²⁺, m/z 310.44 [M+CH₃CO₂]³⁺.



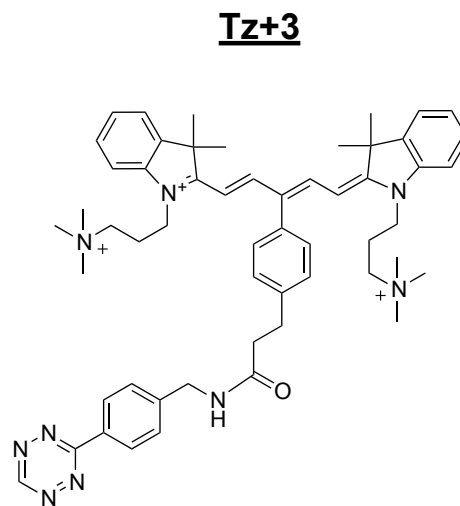
Chemical Formula: $C_{51}H_{54}N_7O_{13}S_4^{3-}$
 Exact Mass: 1100.27



Chemical Formula: $C_{49}H_{52}N_7O_7S_2^-$
 Exact Mass: 914.34



Chemical Formula: $C_{55}H_{68}N_9O_7S_2^+$
 Exact Mass: 1030.47



Chemical Formula: $C_{55}H_{70}N_9O^3+$
 Exact Mass: 872.57

Figure S3. Chemical structures of Tz-fluorophores and their molecular properties.

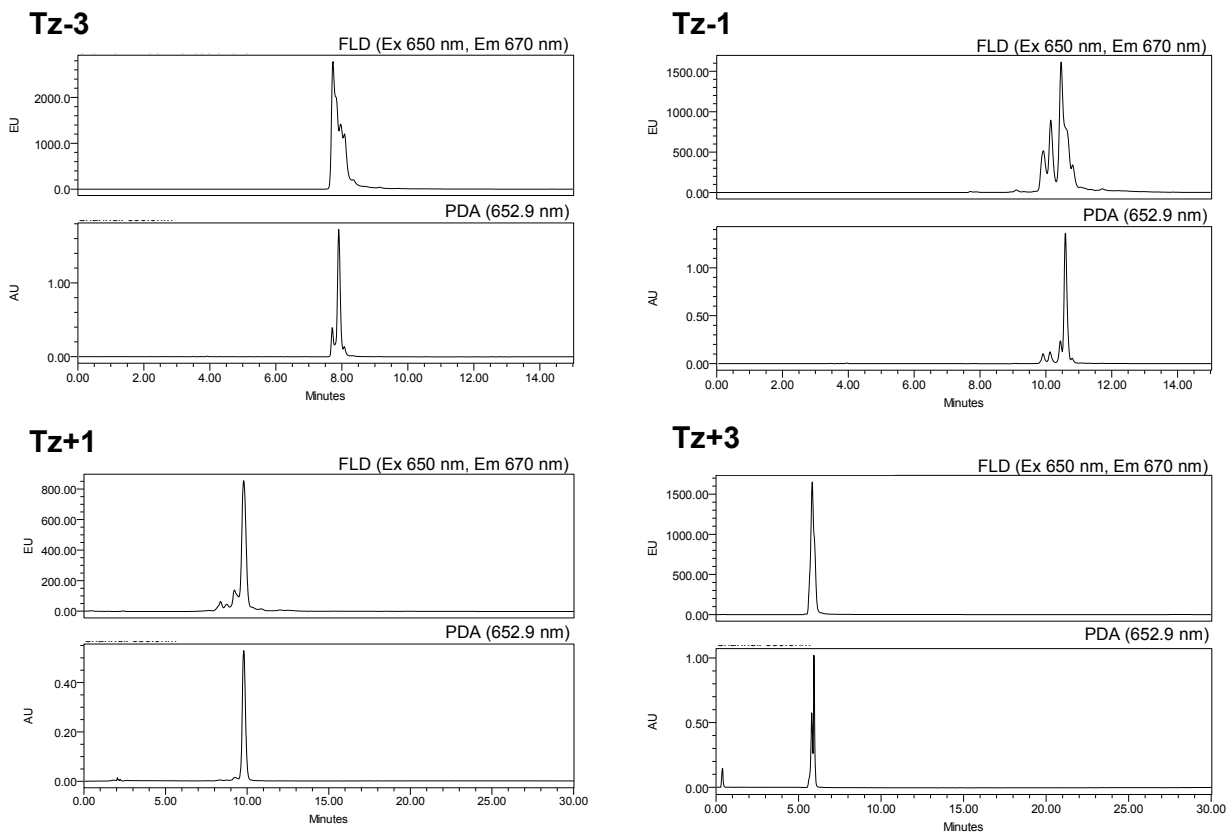


Figure S4. HPLC data for Tz-fluorophores. FLD = fluorescence detector (excitation at 650 nm, emission at 670 nm); PDA = photodiode array.

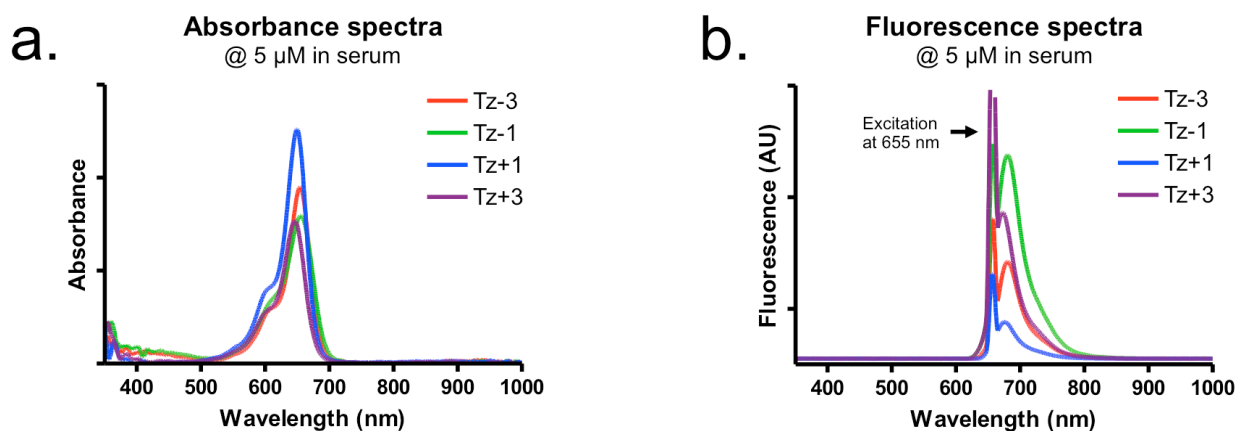


Figure S5. Optical properties of Tz-fluorophores: (a) Absorbance and (b) fluorescence spectra.

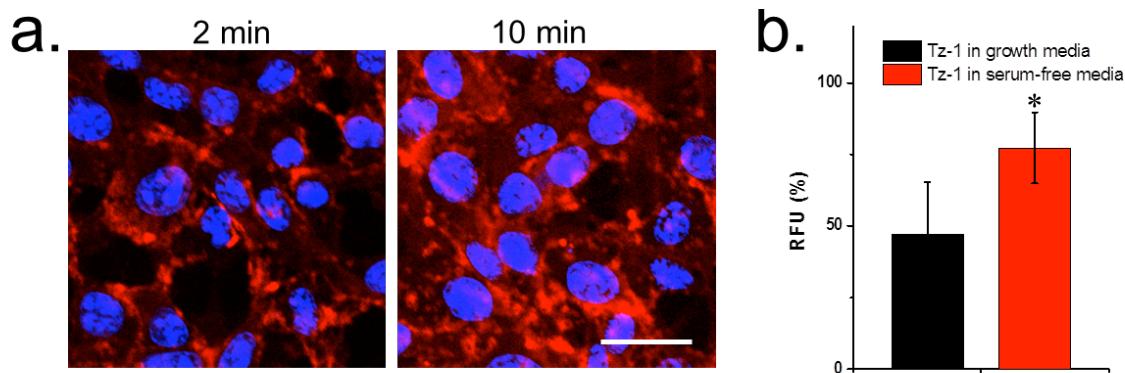


Figure S6. Binding of Tz-1 with TCO-modified cells in serum-free culture media. a) Time-dependent fluorescence images of TCO-modified B16F10 cells bound with Tz-1 in serum-free media. Blue = DAPI; red = 700 nm NIR fluorescence. Scale bar = 10 μ m. b) Fluorescence intensity of Tz-1 bound with TCO-modified B16F10 cells in growth or serum-free media 2 min post-incubation. (n=5, mean \pm s.d., * $P < 0.05$).

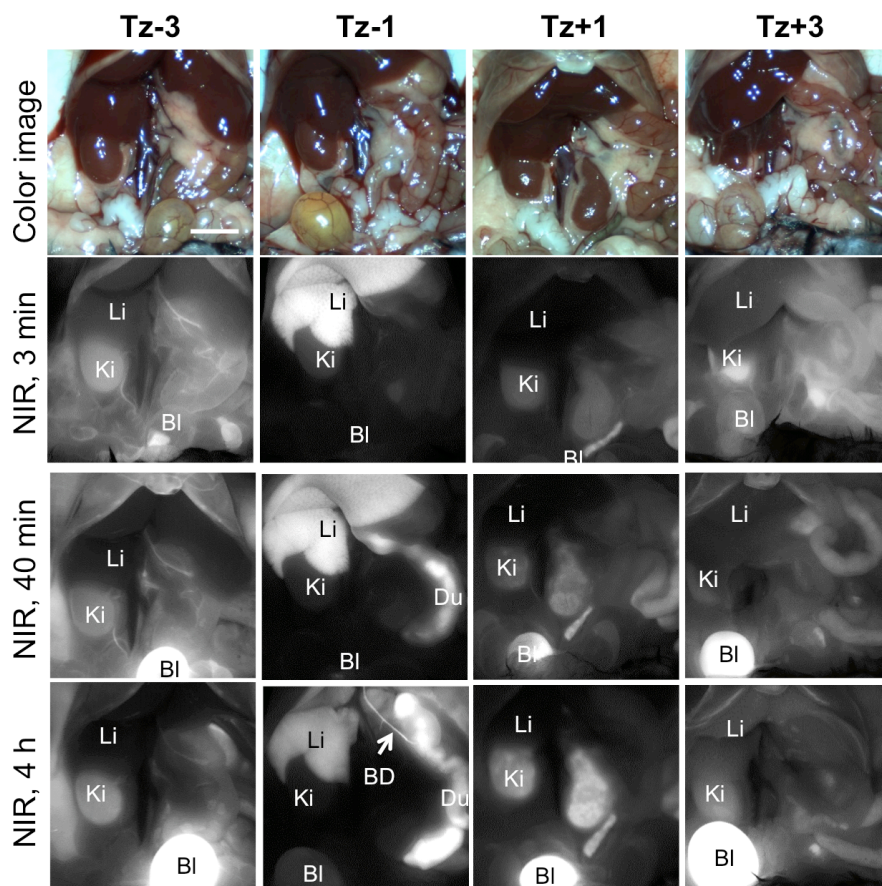


Figure S7. Real-time *in vivo* fluorescence images of the C57BL/6 mice 3, 40, and 240 min post-injection of Tz-fluorophores. Abbreviations used are: Bl, bladder; BD, bile duct; Du, duodenum; Ki, kidney; Li, liver. Scale bar = 1 cm.

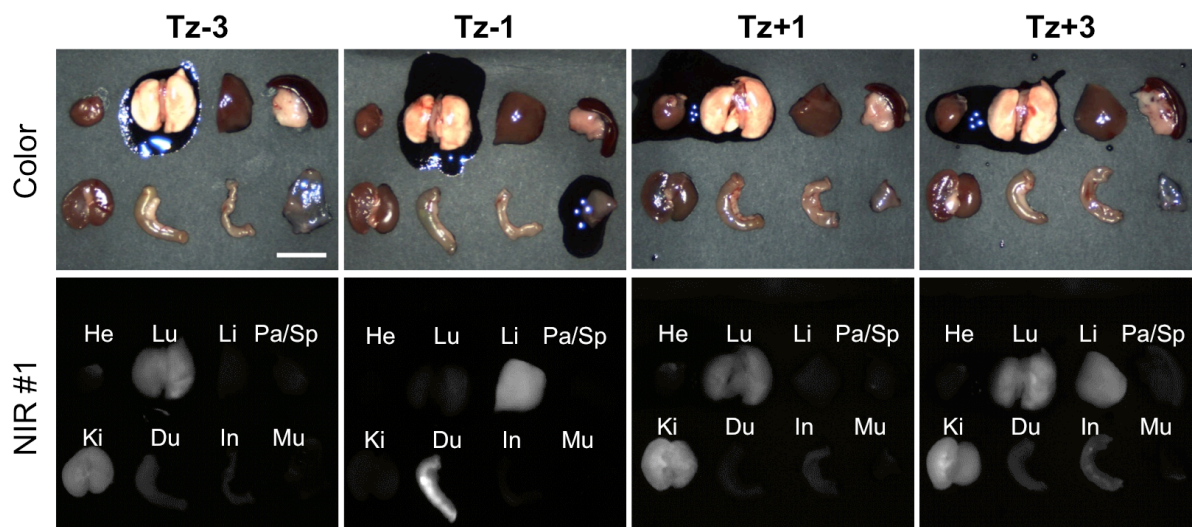


Figure S8. *Ex vivo* fluorescence images of resected organs 4 h post-injection of Tz-fluorophores. Abbreviations used are: Du, duodenum; He, Heart; In, intestine; Ki, kidney; Li, liver; Lu, lungs; Mu, muscle; Pa, pancreas; Sp, spleen. Scale bar = 1 cm.

References

- [1] Owens E, Bruschi N, Tawney JG, Henary M. A microwave-assisted and environmentally benign approach to the synthesis of near infrared fluorescent pentamethine cyanine dyes. *Dyes Pigm.* 2015, 113, 27-37.
- [2] Hyun H, Henary M, Gao T, Narayana L, Owens EA, Alyabyev S, Lee JH, Bordo MW, Park GL, Frangioni JV, Choi HS. 700-nm zwitterionic near-infrared fluorophores for dual-channel image-guided surgery. *Mol Imaging Biol.* 2015. DOI: 10.1007/s11307-015-0870-4.
- [3] Owens E, Hyun H, Kim SH, Lee JH, Park G, Ashitate Y, Choi J, Hong GH, Alyabyev S, Lee SJ, Khang G, Henary M, Choi HS. Highly charged cyanine fluorophores for trafficking scaffold degradation. *Biomed Mater.* 2013; 8(1): 014109.
- [4] Nanjunda R, Owens EA, Mickelson L, Alyabyev S, Kilpatrick N, Wang S, Henary M, Wilson DW. Halogenated pentamethine cyanine dyes exhibiting high fidelity for G-quadruplex DNA. *Bioorg Med Chem.* 2012; 20(24): 7002-11.